

Synergistic Effect of Carbonate Apatite and Autogenous Bone on Osteogenesis

溝上, 宗久

<https://hdl.handle.net/2324/6787526>

出版情報 : Kyushu University, 2022, 博士 (歯学), 課程博士

バージョン :

権利関係 : © 2022 by the authors. Licensee MDPI, Basel, Switzerland. This article is an open access article distributed under the terms and conditions of the Creative Commons Attribution (CC BY) license.

Article

Synergistic Effect of Carbonate Apatite and Autogenous Bone on Osteogenesis

Ikiru Atsuta ^{1,*}, Tokihisa Mizokami ^{2,3}, Yohei Jinno ², Bin Ji ^{1,2}, Tingyu Xie ^{1,2} and Yasunori Ayukawa ²

¹ Division of Advanced Dental Devices and Therapeutics, Faculty of Dental Science, Kyushu University, Fukuoka 8128582, Japan

² Section of Implant and Rehabilitative Dentistry, Division of Oral Rehabilitation, Faculty of Dental Science, Kyushu University, Fukuoka 8128582, Japan

³ Mizokami Dental Office, Fukuoka 8190366, Japan

* Correspondence: atsuta@dent.kyushu-u.ac.jp; Tel.: +81-92-642-6441

Abstract: Bone augmentation using artificial bone is an important option in dental defect prostheses. A bone substitute using carbonate apatite (CO₃Ap), an inorganic component of bone, was reported to have promising bone formation and bone replacement ability. However, the osteoinductivity of artificial bone is less than autogenous bone (AB). In this study, CO₃Ap with AB is demonstrated as a clinically effective bone substitute. For in vitro experiments, an osteoclast-like cell (RAW-D) was cultured in the presence of AB, CO₃Ap, or both (Mix), and the number of osteoclasts was evaluated. Osteoblasts were also cultured under the same conditions, and the number of adherent cells was evaluated. For in vivo experiments, a few holes were created in the rat tibia and AB, CO₃Ap, or Mix were added. At 0, 14, and 21 days, the tissue morphology of the wound area was observed, and the thickness of the cortical bone was measured. In vitro, Mix did not increase the number of osteoclasts or osteoblasts. However, in vivo, the rate of bone replacement remarkably increased with Mix on dome-shape. A bone-grafting material combining osteoinductive AB with abundant artificial bone is expected to be clinically easy to use and able to form bone.



Citation: Atsuta, I.; Mizokami, T.; Jinno, Y.; Ji, B.; Xie, T.; Ayukawa, Y. Synergistic Effect of Carbonate Apatite and Autogenous Bone on Osteogenesis. *Materials* **2022**, *15*, 8100. <https://doi.org/10.3390/ma15228100>

Academic Editor: Artak Heboyan

Received: 11 October 2022

Accepted: 14 November 2022

Published: 16 November 2022

Publisher's Note: MDPI stays neutral with regard to jurisdictional claims in published maps and institutional affiliations.



Copyright: © 2022 by the authors. Licensee MDPI, Basel, Switzerland. This article is an open access article distributed under the terms and conditions of the Creative Commons Attribution (CC BY) license (<https://creativecommons.org/licenses/by/4.0/>).

Keywords: autogenous bone; carbonate apatite; bone-inductive; bone formation; rat tibia

1. Introduction

Insufficient bone volume is a serious problem in dental prosthetic treatments. Jaw-bones resorb rapidly after teeth extraction [1,2]; however, it is important to recover or maintain the bone volume for denture stability, aesthetics of the crown prosthesis, and implant support. As a result, bone substitutes are used. Autogenous bone (AB) is the most widely used bone substitute [3]. However, because AB requires the patient's own bone to be harvested, there are limitations because of invasiveness to the patient and how much can be harvested [4–6]. As a result, artificial bone is a promising alternative to maintain space until the bone is reformed [7,8]. Artificial bone is simply a scaffold for osteoblasts to seed and form bone, i.e., osteoconductivity [9], and artificial bone is slowly replaced by bone as a function of its bone replacement ability [10].

Osteoinduction is a process that supports the body's healing process and acts as a starting point for bone formation [11,12]. Osteoinductivity is the ability to attract mesenchymal stem cells to their surroundings, differentiate the mesenchymal stem cells into osteoblasts, and induce osteogenesis [13]. This behavior is strongly observed in AB with bone marrow [11,14], and rarely observed without bone marrow or with artificial bones [15]. If artificial bone can be endowed with osteoinductivity, the efficiency of bone formation will dramatically increase. Specifically, artificial bone physically inhibits the invasion of soft tissue until new bone is formed, serves as a scaffold for proliferating bone-related cells, and may be an optimal bone-grafting material that can induce bone.

In this study, carbonate apatite (CO₃Ap) was selected as a representative of artificial bone. Some materials for artificial bone remain at the site without being replaced for a long period of time to keep “space making” for bone formation, but there is a risk of infection [16,17]. It is important to have a composition similar to that of bone for biocompatibility. Therefore, an artificial material with a composition similar to that of autogenous bone, such as a bone substitute containing CO₃Ap, which is an inorganic component of bone, has gained clinical attention [18,19]. CO₃Ap is an inorganic component of bone with high osteoconductivity and bone replacement ability. However, CO₃Ap is not osteoinductive like most other bone substitutes [20].

By blending CO₃Ap and AB, CO₃Ap will create the space for bone formation, and the AB will attract mesenchymal stem cells and induce bone formation by differentiating the cells into osteoblasts. Therefore, the advantages of each material are used.

The effect of mixing AB and artificial bone was evaluated using a bone defect in a rat tibia, and the mixture is expected to be clinically easy to use and efficacious in creating new bone.

2. Materials and Methods

2.1. Materials

AB was collected from the femur and tibia of 6-week-old Wistar male rats (different animals than used for the surgery experiments) using a bone scraper (Micros, OKABE, Tokyo, Japan). The collected AB was dried under UV irradiation on a clean bench for two days. Cytrans[®] (CO₃Ap, GC, Tokyo, Japan), a pure CO₃Ap dense granule, was used as the bone substitute [21,22]. The granules were 300–600 µm in diameter.

2.2. Osteoblast and RAW-D Culture

MC3T3-E1 cells were used as an osteoblastic cell line, and they were cultured in α -modified minimum essential medium (α MEM; Wako, Osaka, Japan) with 10% fetal bovine serum (FBS, Thermo Fisher Scientific, Waltham, MA, USA) for four days.

RAW-D cells, an osteoclast precursor cell line, were differentiated to murine osteoclasts as previously described [23,24]. Briefly, RAW-D cells were cultured in α -MEM with 10% FBS in the presence of RANKL (50 ng/mL, ORIENTAL YEAST, Tokyo, Japan) for four days.

The cells (6.8×10^3 /mL) were cultured indirectly with materials using a Transwell[®] insert as a separator [25]. The cells were cultured in the bottom chamber with or without materials (AB, CO₃AP, and AB/CO₃AP) in the upper chamber (a pore size of 200 µm).

2.3. Immunofluorescence Staining

The Cell membrane and Actin filament of the osteoblasts were stained with CellLight Plasma membrane-GFP (Thermo Fisher Scientific) and tetramethylrhodamine isothiocyanate ghost pencil peptide (Chemicon International, Temecula, CA, USA). After staining, the nuclei were stained with VECTASHIELD[®] (Vector Laboratories, Burlingame, CA, USA). The cells stained were observed under fluorescence microscope (BZ-9000, Keyence, Osaka, Japan).

2.4. Tartrate-Resistant acid Phosphatase (TRAP) Activity

The TRAP activity of the RAW-D cells was examined [26]. After four days of incubation, the cells were fixed in 37% formaldehyde (WAKO), permeabilized in ethanol/acetone (WAKO), and observed with a TRAP staining kit (Sigma-Aldrich, St. Louis, MO, USA).

2.5. Cell Counting

The samples were observed with BZ-X800 (KEYENCE). The number of TRAP-positive cells and osteoblast-like cells was counted per well with BZ-X800 Analyzer software (KEYENCE).

2.6. Animals

Wistar rats were cared for under the guidelines of Kyushu University (approval number: A29-222-0). The experimental model followed a previous report [27]. Briefly, bone defects (1.5-mm hole) were created in the right tibia of 6-week-old male rats (30; 120–150 g) using a dental round bur, and AB, CO₃Ap, or their mixture (Mix) were used to fill the defects with 1.2 mm diameter NIET carrier (Japan dental supply, Tokyo, Japan). The carrier was used twice to keep the volume of the material in the defect constant. Bone-grafting material was added to form a dome over the defect, and healing was observed after fixation with a membrane (Cytrans Elashield; GC) and two sutures (4-0 Softretch; GC). The control group was allowed to heal without additional material. The rats were sacrificed via anesthesia after 14 or 21 days, and samples were created. Samples from animals sacrificed immediately after making the holes were considered Day 0.

2.7. Tissue Preparation

Tissues for hematoxylin and eosin (HE) staining were prepared as previously described [28–30]. Briefly, the samples were removed from the rats, fixed in 4% paraformaldehyde for 24 h, and then preserved in Kalkitox (FUJIFILM Wako Pure Chemical, Osaka, Japan) at 4 °C for 18 h. Sagittal sections (10 µm thick) were cut using a cryostat and stained with HE.

2.8. Bone Thickness

The vertical length of cortical bone on the bone marrow was considered the bone thickness. The anteroposterior position for the measurement was located by the central part of the hole and it was measured using a BZ-X800 microscope (KEYENCE).

2.9. Statistical Analysis

All measurements were performed 3 times by 3 people, and the average values were graphed. Data are expressed as means ± standard deviation (SD). One-way analysis of variance with Scheffe's post hoc was performed. $p < 0.05$ values were considered significant.

3. Results

3.1. Effects of the Bone Substitute on Osteogenic Cells

As shown in Figure 1, a cell culture experiment was performed to confirm whether the proliferation of osteoblasts and the ability to differentiate into osteoclasts were affected by the bone substitute. In addition to the three groups of bone substitute (bone alone (AB group), carbonate apatite alone (CO₃Ap group), and a mixture of AB and CO₃Ap (Mix group)), a control was prepared without material (Cont group) and cultured for four days. The CO₃Ap group showed less osteoblast proliferation than the control group and Mix group, and less osteoclast differentiation than the AB group.

3.2. Effects of the Bone Substitute on Bone Healing

Using the animal experimental model shown in Figure 2, morphological images were observed after 14 and 21 days, as shown in Figure 3. Figure 3b shows an image in which the cortical bone was perforated with a round bar. A section was prepared parallel to the long axis, and the cortical bone was completely lost at a width of 1.0 mm. The bone marrow was penetrated. As shown in Figure 3c, bone closure occurred even in the control at Day 14; although there were traces of the defect, the closure was complete at Day 21. In the AB group, after 14 days, the AB remained, similar to a foreign substance; however, after 21 days, the cortical bone was thicker than that in the control group. In the CO₃Ap group, the material clearly remained even after 21 days; however, the surrounding area was covered with mature bone. In the Mix group, material remained as in the CO₃Ap group; however, thick bone incorporating the AB was formed.

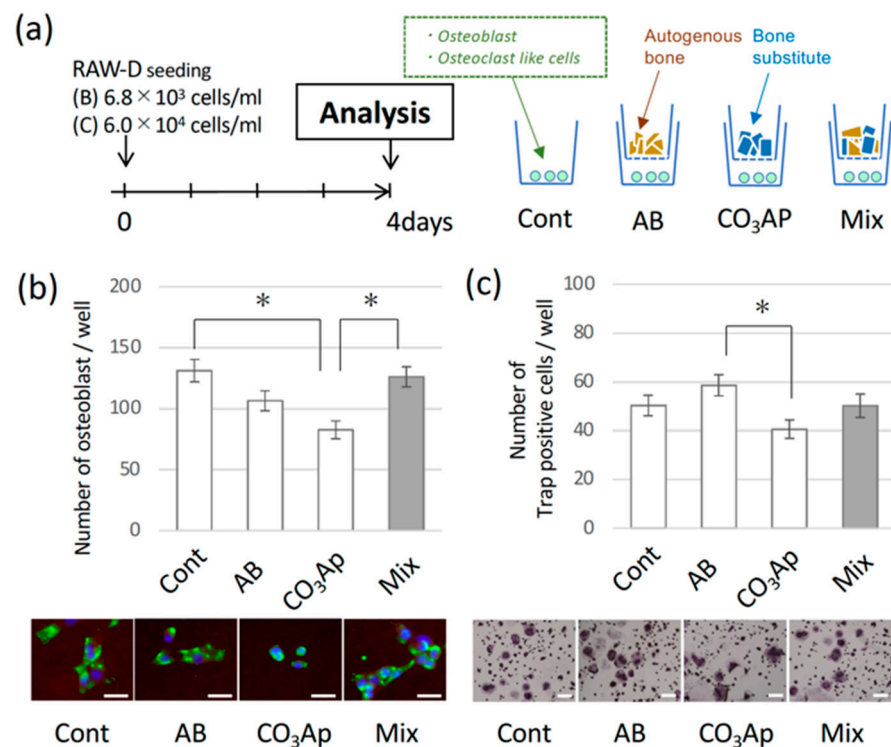


Figure 1. (a) Culture protocol. Osteoblasts from the rat bone marrow of a tibia were used, and RAW-D cells were used as osteoclast precursor cells. Autogenous bone (AB), carbonate apatite (CO₃AP), and a mixture of AB and CO₃AP (Mix) were placed in the upper well of a Transwell, and nothing was added to the control group (Cont). (b) Number of adhered osteoblasts after four days. Scale bar = 20 μm. (c) The number of TRAP-positive cells representing cells differentiated into osteoclasts. (* *p* < 0.05) Scale bar = 20 μm.

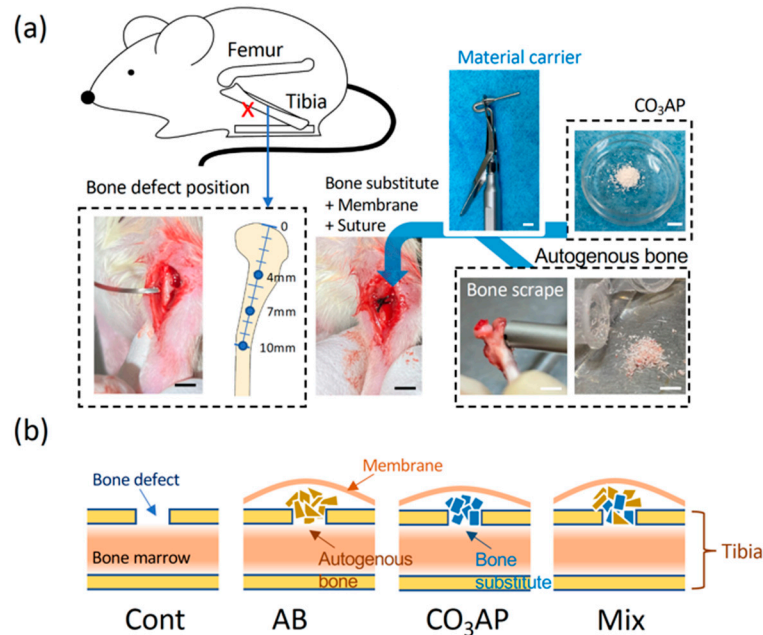


Figure 2. (a) Tibia defect and preparation of autogenous bone. A hole was created in the tibia (red X) using a round bur, material was inserted using a filling tool (material carrier), and the hole was covered with a membrane and two sutures. Scale bar = 5 mm. (b) Experimental group. For the control, nothing was inserted into the tibia hole. In the autologous group, a separate dry tibia was used. In the Mix group, a 1:1 volume of scraped bone and CO₃AP was used to fill the hole.

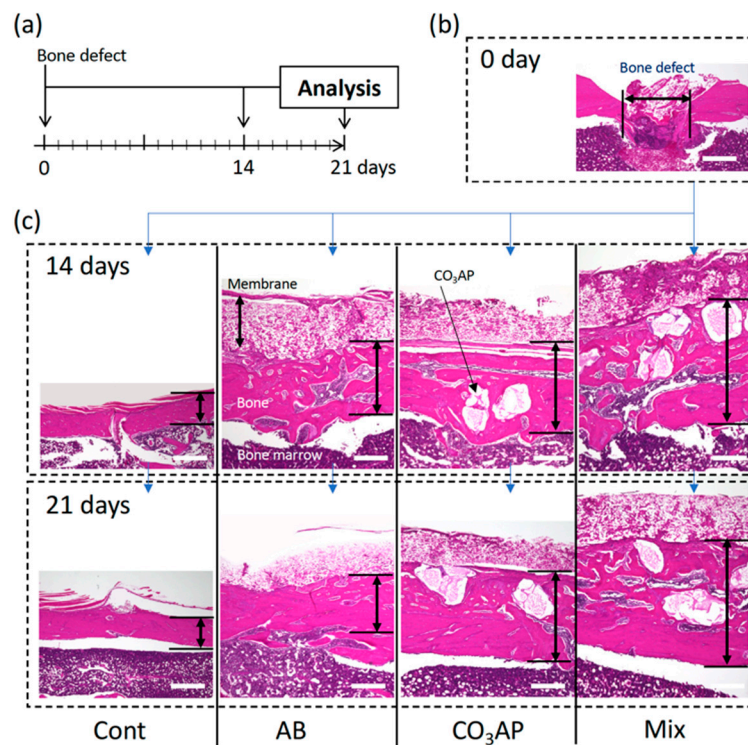


Figure 3. (a) Animal protocol. (b) Photograph of the morphology immediately after creating a bone defect in the tibia (Day 0). (c) Osteogenic process. Hematoxylin and eosin staining after 14 days and 21 days in the control group (Cont), autogenous bone group (AB), carbonate apatite group (CO₃AP), and AB and CO₃AP mixed group (Mix). Scale bar = 100 μ m.

Figure 4 shows the thickness of the bone. After 14 days, the thickness was maintained only in the Mix group. After 21 days, the thickness in the control group was significantly less than that in the CO₃AP and Mix groups.

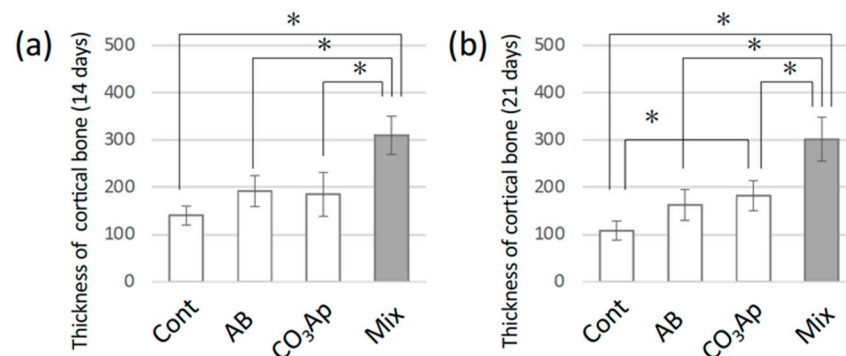


Figure 4. Thickness of the injured bone (a) 14 days and (b) 21 days after surgery (* $p < 0.05$) for the control group (Cont), autogenous bone group (AB), carbonate apatite group (CO₃AP), and AB and CO₃AP mixed group (Mix).

4. Discussion

When bone has a defect because of trauma, such as a fracture, the edge of the bone facing the defect is destroyed by osteoclasts, and bone formation-related cells, such as osteoblasts, migrate into the defect [31,32]. The defect is then filled with a collagen-like structure, and the bone is closed by inorganic material deposition [33,34]. However, because bone closure is slower than that of soft tissue growth, in many cases, soft tissue enters or presses the space where the bone should heal, thereby blocking bone healing [35,36]. Therefore, the bone substitute serves as a framework to secure a space for bone formation,

and functions as a scaffold for osteogenic-related cells that migrate to the defect site to differentiate and secrete collagen. Additional important functions of material are an absorption speed to maintain space until bone formation progresses [7], cell affinity [37], and absorbability to allow for bone replacement [38].

Osteoinductivity to support osteogenesis is also an important material characteristic. The progression of bone formation from the site contacting the bone is general healing; however, with time, resorption of distant sites will occur. Therefore, it may be difficult to create bone with a significant thickness. Alternatively, if the material has osteoinductivity, bone formation will occur at the part facing the bone and from where the material is placed. Therefore, bone replacement will proceed faster and more efficiently, potentially reducing the risk that soft tissue invades the area.

However, AB with bone marrow is an outstanding material with osteoinductivity [39,40]. Although dried bone is clearly inferior to freshly harvested AB, it still has osteoinductivity [41,42].

As shown in Figure 2, a hole was created in the tibia, bone-grafting material was added to form a dome over the hole, and healing was observed after fixation with a membrane. Although a larger bone defect is necessary, the defect size was similar to that in other reports [11,39,43]. The healing period was approximately 14 days, even in the control group without bone substitute, and bone closure was observed in all experimental groups. However, as shown in Figure 3, the quality and volume of bone differed greatly. In the AB group, mature bone similar to that in the control group was formed after 14 and 21 days (Figure 3c). Alternatively, as shown in Figure 4, the thickness of the bone in the groups with CO₃Ap was greater than that in the control group. A large volume of bone was formed because of the bulkiness of the material, and the cortical bone seemed to be thicker. After 21 days, there was a significant difference compared with the control group (Figure 4b). Moreover, in the Mix group with CO₃Ap and AB, bone formation occurred over a large area that spread vertically, indicating that space-making and bone formation occurred at the same time. As shown in Figure 4a,b, a strong increase in vertical bone was observed in the Mix group, indicating optimal osteoinduction near the space-making artificial material.

However, it is unlikely that the material leached out and induced osteogenesis. As shown in Figure 1, when bones and materials were cultured at the same time using a Transwell without direct contact, the presence of the bone substitute did not significantly increase osteoblast proliferation or osteoclast differentiation compared with the control group. With CO₃Ap, the proliferation of osteoblasts was significantly less than that of the control group (Figure 1a), and the proliferation of osteoclasts was less than that of the AB group (Figure 1b). CO₃Ap elutes calcium in vivo [14,16]. Alternatively, the osteoblast proliferation and osteoclast differentiation increased with an increase in calcium concentration [44,45]. However, CO₃Ap actually adsorbs calcium from a solution with high calcium concentration [46]. Specifically, in our recent study, we measured the calcium concentration in the culture medium, and found that the concentration decreased (data not shown).

There is a difference between cell culture conditions and an in vivo environment; however, rather than the material itself promoting osteogenesis, AB induced osteogenesis-related cells around CO₃Ap. Future studies will clarify which factors induce such cells around the material, and they will be added to develop a novel bone substitute with further improved osteoinductivity.

5. Conclusions

A mixture of CO₃Ap and AB takes advantage of the osteogenic and osteoinductive properties of each component, which may create reliable bone formation over a wide area.

Author Contributions: Conceptualization, T.M. and I.A.; methodology, I.A. and Y.J.; validation, I.A.; formal analysis, I.A., T.M. and Y.J.; investigation, I.A.; resources, T.M. and I.A.; writing—original draft preparation, I.A.; writing—review and editing, I.A., B.J. and T.X.; visualization, Y.J. and T.M.; supervision, Y.J. and Y.A.; project administration, Y.A. All authors have read and agreed to the published version of the manuscript.

Funding: This research received no external funding.

Institutional Review Board Statement: Our in vivo and in vitro study were approved by the guidelines established by Kyushu University (approval number: A29-222-0).

Data Availability Statement: The data presented in this study are available on request from the corresponding author.

Acknowledgments: The first author would like to express their sincere thanks to colleagues in our division for composing this review article.

Conflicts of Interest: I.A. belongs to the Division of Advanced Dental Devices and Therapeutics, Faculty of Dental Science, Kyushu University. This division is endowed by GC Corporation, Tokyo, Japan. GC Corporation had no specific roles in the conceptualization, design, data collection, analysis, decision to publish, or preparation of the manuscript. All other authors declare that they have no competing interests.

References

1. Pietrokovski, J.; Massler, M. Alveolar ridge resorption following tooth extraction. *J. Prosthet Dent.* **1967**, *17*, 21–27. [[CrossRef](#)]
2. Schropp, L.; Wenzel, A.; Kostopoulos, L.; Karring, T. Bone healing and soft tissue contour changes following single-tooth extraction: A clinical and radiographic 12-month prospective study. *Int. J. Periodontics Restor. Dent.* **2003**, *23*, 313–323.
3. Kumar, P.; Vinitha, B.; Fathima, G. Bone grafts in dentistry. *J. Pharm. Bioallied. Sci.* **2013**, *5*, 125–127. [[CrossRef](#)]
4. Dimitriou, R.; Jones, E.; McGonagle, D.; Giannoudis, P.V. Bone regeneration: Current concepts and future directions. *BMC Med.* **2011**, *9*, 66. [[CrossRef](#)]
5. Nkenke, E.; Neukam, F.W. Autogenous bone harvesting and grafting in advanced jaw resorption: Morbidity, resorption and implant survival. *Eur. J. Oral Implantol.* **2014**, *7*, 203–217.
6. Misch, C.M. Comparison of intraoral donor sites for onlay grafting prior to implant placement. *Int. J. Oral Maxillofac. Implants.* **1997**, *12*, 767–776.
7. Polo-Corrales, L.; Latorre-Esteves, M.; Ramirez-Vick, J.E. Scaffold design for bone regeneration. *J. Nanosci. Nanotechnol.* **2014**, *14*, 15–56. [[CrossRef](#)]
8. Poh, P.S.P.; Valanis, D.; Bhattacharya, K.; van Griensven, M.; Dondl, P. Optimization of Bone Scaffold Porosity Distributions. *Sci. Rep.* **2019**, *9*, 9170. [[CrossRef](#)]
9. Sheikh, Z.; Hamdan, N.; Ikeda, Y.; Grynypas, M.; Ganss, B.; Glogauer, M. Natural graft tissues and synthetic biomaterials for periodontal and alveolar bone reconstructive applications: A review. *Biomater. Res.* **2017**, *21*, 9. [[CrossRef](#)] [[PubMed](#)]
10. Titsinides, S.; Agrogiannis, G.; Karatzas, T. Bone grafting materials in dentoalveolar reconstruction: A comprehensive review. *Jpn. Dent. Sci Rev.* **2019**, *55*, 26–32. [[CrossRef](#)] [[PubMed](#)]
11. Miron, R.J.; Hedbom, E.; Saulacic, N.; Zhang, Y.; Sculean, A.; Bosshardt, D.D.; Buser, D. Osteogenic potential of autogenous bone grafts harvested with four different surgical techniques. *J. Dent. Res.* **2011**, *90*, 1428–1433. [[CrossRef](#)] [[PubMed](#)]
12. Habibovic, P.; Sees, T.M.; van den Doel, M.A.; van Blitterswijk, C.A.; de Groot, K. Osteoinduction by biomaterials—physicochemical and structural influences. *J. Biomed. Mater. Res. A* **2006**, *77*, 747–762. [[CrossRef](#)] [[PubMed](#)]
13. Albrektsson, T.; Johansson, C. Osteoinduction, osteoconduction and osseointegration. *Eur. Spine J.* **2001**, *10* (Suppl. S2), S96–S101.
14. Ishikawa, K.; Hayashi, K. Carbonate apatite artificial bone. *Sci. Technol. Adv. Mater.* **2021**, *22*, 683–694. [[CrossRef](#)]
15. Habibovic, P.; Kruyt, M.C.; Juhl, M.V.; Clyens, S.; Martinetti, R.; Dolcini, L.; Theilgaard, N.; van Blitterswijk, C.A. Comparative in vivo study of six hydroxyapatite-based bone graft substitutes. *J. Orthop. Res.* **2008**, *26*, 1363–1370. [[CrossRef](#)] [[PubMed](#)]
16. Velard, F.; Schlaubitz, S.; Fricain, J.C.; Guillaume, C.; Laurent-Maquin, D.; Moller-Siegert, J.; Vidal, L.; Jallot, E.; Sayen, S.; Raissle, O.; et al. In vitro and in vivo evaluation of the inflammatory potential of various nanoporous hydroxyapatite biomaterials. *Nanomedicine* **2015**, *10*, 785–802. [[CrossRef](#)]
17. Goto, T.; Kojima, T.; Iijima, T.; Yokokura, S.; Kawano, H.; Yamamoto, A.; Matsuda, K. Resorption of synthetic porous hydroxyapatite and replacement by newly formed bone. *J. Orthop. Sci.* **2001**, *6*, 444–447. [[CrossRef](#)]
18. Fujisawa, K.; Akita, K.; Fukuda, N.; Kamada, K.; Kudoh, T.; Ohe, G.; Mano, T.; Tsuru, K.; Ishikawa, K.; Miyamoto, Y. Compositional and histological comparison of carbonate apatite fabricated by dissolution-precipitation reaction and Bio-Oss((R)). *J. Mater. Sci. Mater. Med.* **2018**, *29*, 121. [[CrossRef](#)]
19. Kudoh, K.; Fukuda, N.; Kasugai, S.; Tachikawa, N.; Koyano, K.; Matsushita, Y.; Ogino, Y.; Ishikawa, K.; Miyamoto, Y. Maxillary Sinus Floor Augmentation Using Low-Crystalline Carbonate Apatite Granules With Simultaneous Implant Installation: First-in-Human Clinical Trial. *J. Oral Maxillofac. Surg.* **2019**, *77*, 985.e1–985.e11. [[CrossRef](#)]
20. Ishikawa, K.; Kawachi, G.; Tsuru, K.; Yoshimoto, A. Fabrication of calcite blocks from gypsum blocks by compositional transformation based on dissolution-precipitation reactions in sodium carbonate solution. *Mater. Sci. Eng. C Mater. Biol. Appl.* **2017**, *72*, 389–393. [[CrossRef](#)]
21. Lin, X.; Matsuya, S.; Nakagawa, M.; Terada, Y.; Ishikawa, K. Effect of molding pressure on fabrication of low-crystalline calcite block. *J. Mater. Sci Mater. Med.* **2008**, *19*, 479–484. [[CrossRef](#)]

22. Wakae, H.; Takeuchi, A.; Udoh, K.; Matsuya, S.; Munar, M.L.; LeGeros, R.Z.; Nakasima, A.; Ishikawa, K. Fabrication of macroporous carbonate apatite foam by hydrothermal conversion of alpha-tricalcium phosphate in carbonate solutions. *J. Biomed. Mater. Res. A* **2008**, *87*, 957–963. [[CrossRef](#)] [[PubMed](#)]
23. Kukita, T.; Wada, N.; Kukita, A.; Kakimoto, T.; Sandra, F.; Toh, K.; Nagata, K.; Iijima, T.; Horiuchi, M.; Matsusaki, H.; et al. RANKL-induced DC-STAMP is essential for osteoclastogenesis. *J. Exp. Med.* **2004**, *200*, 941–946. [[CrossRef](#)] [[PubMed](#)]
24. Watanabe, T.; Kukita, T.; Kukita, A.; Wada, N.; Toh, K.; Nagata, K.; Nomiya, H.; Iijima, T. Direct stimulation of osteoclastogenesis by MIP-1alpha: Evidence obtained from studies using RAW264 cell clone highly responsive to RANKL. *J. Endocrinol.* **2004**, *180*, 193–201. [[CrossRef](#)]
25. Egashira, Y.; Atsuta, I.; Narimatsu, I.; Zhang, X.; Takahashi, R.; Koyano, K.; Ayukawa, Y. Effect of carbonate apatite as a bone substitute on oral mucosal healing in a rat extraction socket: In vitro and in vivo analyses using carbonate apatite. *Int. J. Implant. Dent.* **2022**, *8*, 11. [[CrossRef](#)]
26. Takemura, Y.; Moriyama, Y.; Ayukawa, Y.; Kurata, K.; Rakhmatia, Y.D.; Koyano, K. Mechanical loading induced osteocyte apoptosis and connexin 43 expression in three-dimensional cell culture and dental implant model. *J. Biomed. Mater. Res. A* **2019**, *107*, 815–827. [[CrossRef](#)]
27. Moriyama, Y.; Ayukawa, Y.; Ogino, Y.; Atsuta, I.; Todo, M.; Takao, Y.; Koyano, K. Local application of fluvastatin improves peri-implant bone quantity and mechanical properties: A rodent study. *Acta Biomater.* **2010**, *6*, 1610–1618. [[CrossRef](#)] [[PubMed](#)]
28. Atsuta, I.; Ayukawa, Y.; Furuhashi, A.; Narimatsu, I.; Kondo, R.; Oshiro, W.; Koyano, K. Epithelial sealing effectiveness against titanium or zirconia implants surface. *J. Biomed. Mater. Res. A* **2019**, *107*, 1379–1385. [[CrossRef](#)]
29. Atsuta, I.; Yamaza, T.; Yoshinari, M.; Goto, T.; Kido, M.A.; Kagiya, T.; Mino, S.; Shimono, M.; Tanaka, T. Ultrastructural localization of laminin-5 (gamma2 chain) in the rat peri-implant oral mucosa around a titanium-dental implant by immuno-electron microscopy. *Biomaterials* **2005**, *26*, 6280–6287. [[CrossRef](#)]
30. Oshiro, W.; Ayukawa, Y.; Atsuta, I.; Furuhashi, A.; Yamazoe, J.; Kondo, R.; Sakaguchi, M.; Matsuura, Y.; Tsukiyama, Y.; Koyano, K. Effects of CaCl₂ hydrothermal treatment of titanium implant surfaces on early epithelial sealing. *Colloids Surf. B Biointerfaces* **2015**, *131*, 141–147. [[CrossRef](#)]
31. Tang, Y.; Wu, X.; Lei, W.; Pang, L.; Wan, C.; Shi, Z.; Zhao, L.; Nagy, T.R.; Peng, X.; Hu, J.; et al. TGF-beta1-induced migration of bone mesenchymal stem cells couples bone resorption with formation. *Nat. Med.* **2009**, *15*, 757–765. [[CrossRef](#)]
32. Su, P.; Tian, Y.; Yang, C.; Ma, X.; Wang, X.; Pei, J.; Zhao, L.; Nagy, T.R.; Peng, X.; Hu, J.; et al. Mesenchymal Stem Cell Migration during Bone Formation and Bone Diseases Therapy. *Int. J. Mol. Sci.* **2018**, *19*, 2343. [[CrossRef](#)] [[PubMed](#)]
33. Bigham-Sadegh, A.; Oryan, A. Basic concepts regarding fracture healing and the current options and future directions in managing bone fractures. *Int. Wound J.* **2015**, *12*, 238–247. [[CrossRef](#)] [[PubMed](#)]
34. Papachristou, D.J.; Georgopoulos, S.; Giannoudis, P.V.; Panagiotopoulos, E. Insights into the Cellular and Molecular Mechanisms That Govern the Fracture-Healing Process: A Narrative Review. *J. Clin. Med.* **2021**, *10*, 3554. [[CrossRef](#)] [[PubMed](#)]
35. Dahlin, C.; Linde, A.; Gottlow, J.; Nyman, S. Healing of bone defects by guided tissue regeneration. *Plast. Reconstr. Surg.* **1988**, *81*, 672–676. [[CrossRef](#)]
36. Mirhadi, S.; Ashwood, N.; Karagkevrekis, B. Factors influencing fracture healing. *Trauma* **2013**, *15*, 140–155. [[CrossRef](#)]
37. Amini, A.R.; Laurencin, C.T.; Nukavarapu, S.P. Bone tissue engineering: Recent advances and challenges. *Crit. Rev. Biomed. Eng.* **2012**, *40*, 363–408. [[CrossRef](#)]
38. Roden, R.D., Jr. Principles of bone grafting. *Oral Maxillofac. Surg. Clin. N. Am.* **2010**, *22*, 295–300. [[CrossRef](#)]
39. Giannoudis, P.V.; Dinopoulos, H.; Tsiroidis, E. Bone substitutes: An update. *Injury* **2005**, *36* (Suppl. S3), S20-7. [[CrossRef](#)]
40. Niu, C.C.; Tsai, T.T.; Fu, T.S.; Lai, P.L.; Chen, L.H.; Chen, W.J. A comparison of posterolateral lumbar fusion comparing autograft, autogenous laminectomy bone with bone marrow aspirate, and calcium sulphate with bone marrow aspirate: A prospective randomized study. *Spine* **2009**, *34*, 2715–2719. [[CrossRef](#)]
41. Finkemeier, C.G. Bone-grafting and bone-graft substitutes. *J. Bone Joint. Surg. Am.* **2002**, *84*, 454–464. [[CrossRef](#)]
42. Garcia-Gareta, E.; Coathup, M.J.; Blunn, G.W. Osteoinduction of bone grafting materials for bone repair and regeneration. *Bone* **2015**, *81*, 112–121. [[CrossRef](#)]
43. Miron, R.J.; Sculean, A.; Shuang, Y.; Bosshardt, D.D.; Gruber, R.; Buser, D.; Chandad, F.; Zhang, Y. Osteoinductive potential of a novel biphasic calcium phosphate bone graft in comparison with autographs, xenografts, and DFDBA. *Clin Oral Implant. Res.* **2016**, *27*, 668–675. [[CrossRef](#)]
44. Dvorak, M.M.; Siddiqua, A.; Ward, D.T.; Carter, D.H.; Dallas, S.L.; Nemeth, E.F.; Riccardi, D. Physiological changes in extracellular calcium concentration directly control osteoblast function in the absence of calciotropic hormones. *Proc. Natl. Acad. Sci. USA* **2004**, *101*, 5140–5145. [[CrossRef](#)]
45. Maeno, S.; Niki, Y.; Matsumoto, H.; Morioka, H.; Yatabe, T.; Funayama, A.; Toyama, Y.; Taguchi, T.; Tanaka, J. The effect of calcium ion concentration on osteoblast viability, proliferation and differentiation in monolayer and 3D culture. *Biomaterials* **2005**, *26*, 4847–4855. [[CrossRef](#)]
46. Hwang, S.Y.; Putney, J.W., Jr. Calcium signaling in osteoclasts. *Biochim. Biophys. Acta* **2011**, *1813*, 979–983. [[CrossRef](#)]